

GAMMA-RAY-BASED METHOD FOR DENSITY SENSING IN PIPES - EVALUATION OF MEASUREMENT AND DATA PROCESSING

Jan Krupička¹ & Václav Matoušek¹

¹Institute of Hydrodynamics, Academy of Sciences, Czech Republic, Pod Patankou 30/5, 166 00 Prague 6

E-mail: krupicka@ih.cas.cz

Abstract

The paper summarizes our experience with the radiometric devices installed to the experimental pipe loop for investigations of slurry flows in the Institute of Hydrodynamics in Prague. The vertical shifting support and a horizontally collimated beam enable to acquire vertical profiles of chord-averaged densities in a cross section of a pipe transporting a heterogeneous mixture. Moreover, our devices are equipped also with a rotating support. This enables us to acquire data that can be processed by computer tomography algorithms to obtain a distribution of local densities in a pipe cross section. Due to the simple “one source – one detector” construction of our device the number measurement available over a reasonably long time period is limited. Two algorithms for density distribution reconstruction are compared showing their efficiency when dealing with a limited number of data. Numerical simulations show that the accuracy of the method is mainly reduced by the errors in beam positioning, and by randomly generated fluctuations of emission and detection of gamma-ray photons.

Introduction

Investigation of inner structure of flow carrying large amount of settling particles is essential for development and validation of physically based models of sediment laden flow. Such models find their application in steep open channels with erodible bed as well as in pressurized pipes designed for conveying settling slurry. Velocity distribution and distribution of concentration of solid phase in mixture have to be measured to give a picture of a complex structure of the flow.

There are many possibilities how to measure concentration (e.g. sampling, electrical conductivity based methods, optical methods, ultrasound based methods and others). We use radiometric method based on attenuation of gamma ray intensity along gamma-ray beam when passing through the pipe cross-section. As the gamma-ray represents the most energetic electromagnetic radiation, it penetrates deep into the objects and enables investigation of bigger and denser objects than X-ray well-known from medical applications.

If the attenuation is defined as a ratio of incident and passed gamma ray intensity I/I_0 its value is given by the well known exponential equation (1), where L is the length of the beam within the investigated matter and μ is the attenuation coefficient corresponding with the atomic structure and density of investigated matter. Thus the density can be evaluated from measured attenuation using calibration made with the same material as that used in experiment.

$$I/I_0 = e^{-\int \mu \cdot dL} \quad (1)$$

This method was successfully applied in slurry pipe experimental loops in the past (e.g. Pugh 1995, Matoušek, 1997). A device with the source on one side and the detector on the opposite side of a pipe was used in these investigations. Shifting of a source-detector position enabled to acquire a vertical profile of chord-averaged densities from which a concentration profile can be evaluated. More complex configurations were used in other research- and industrial applications (e.g. Lee, Jung, Kim, 2009, Hampel et al, 2007, Hjertaker & Johansen, 2008). These devices often use more than one detector and source to obtain several measurements along different projections in a short time. Such data can be processed by computer tomography algorithms to evaluate a distribution of local densities and concentrations in a pipe section. Przewlocki et al, 1979, used a device with one source and one detector mounted on the liner positioning drive which can be rotated round the pipe centre. They were thus able to obtain similar data as in the case of several detectors but within somewhat longer measuring time. Recently reconstructed pipe loop at Institute of hydrodynamics in Prague was equipped by two radiometric devices of the same type as Przewlocki et al. used.

Experimental facility

Experimental test loop

A major reconstruction of the experimental loop for slurry flow investigation (see Figure 1) took place at the Institute of Hydrodynamics in Prague in 2009. The new loop is made from stainless steel pipes of the inner diameter of

$D=100\text{ mm}$. Instrumentation of the loop allows us to collect data on flow rate, average delivered concentration and pressure losses in horizontal, vertical and tiltable section. Radiometric devices can be mounted to all three sections. For more details on the experimental facility see e.g. Krupička & Matoušek, 2011.

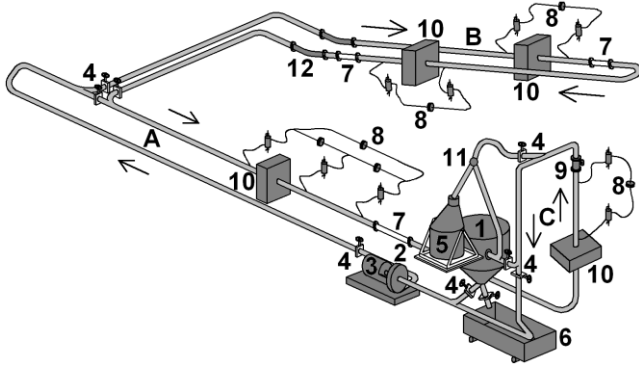


Figure 1: Experimental test loop at Institute of Hydrodynamics in Prague. A – horizontal section, B – tiltable section, C – vertical section, 1 – sump tank, 2 – centrifugal pump, 3 – electric motor, 4 – slide valves, 5 – sampling tank, 6 – slurry reservoir, 7 – glass observation section, 8 – differential pressure meters, 9 – Electromagnetic flow meter, 10 – positions of radiometric devices, 11 – flow divider, 12 – flexible tubes.

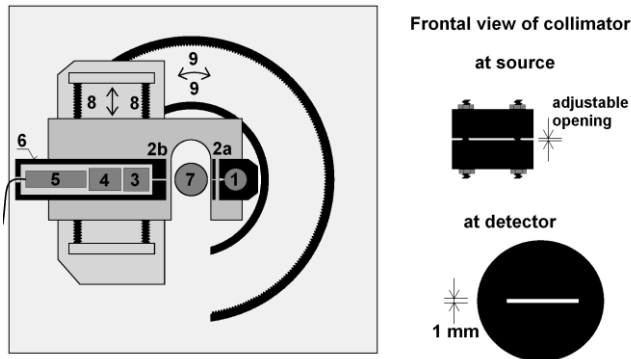


Figure 2: Scheme of radiometric device at Institute of hydrodynamics in Prague. 1 – gamma ray source, 2a – collimator at source, 2b – collimator at detector, 3 – scintillator, 4 – photomultiplier, 5 – multichannel digital analyser, 6 – lead shielding of detector, 7 – pipe cross section, 8 – linear positioning drive, 9 – radial positioning drive.

Radiometric devices

Both of the radiometric devices have the same construction (see Fig. 2). Main components are a gamma-ray source (Cesium Cs-137, activity 740 MBq) on one side and a detector on the opposite side of the pipe. The detector is composed of a scintillating crystal of NaI(Tl) to convert photons of gamma ray to showers of photons of lower energy. These photons invoke electrical response in adjoining photomultiplier. A multichannel digital analyzer

sorts detected pulses according to energy providing energetic spectra of incident gamma-ray. Lead plate with 1 mm wide opening is used to collimate gamma-ray beam at detector. This ensures sufficient spatial resolution of measurement. Moreover, lead collimator with adjustable opening at source was tested to increase the resolution and to suppress the effect of scattered photons.

The source-detector position below or above pipe centre can be shifted by a linear positioning drive providing parallel projections data. These data result in chord averaged density and concentration profiles. Radial positioning drive enables the support of linear positioning drive to rotate round the pipe centre and to acquire parallel projections at different inclinations. The linear positioning drive is controlled by the computer according to the predefined table of positions so the parallel projection data are acquired in a fully automatic way. Radial positioning drive has to be handled manually.

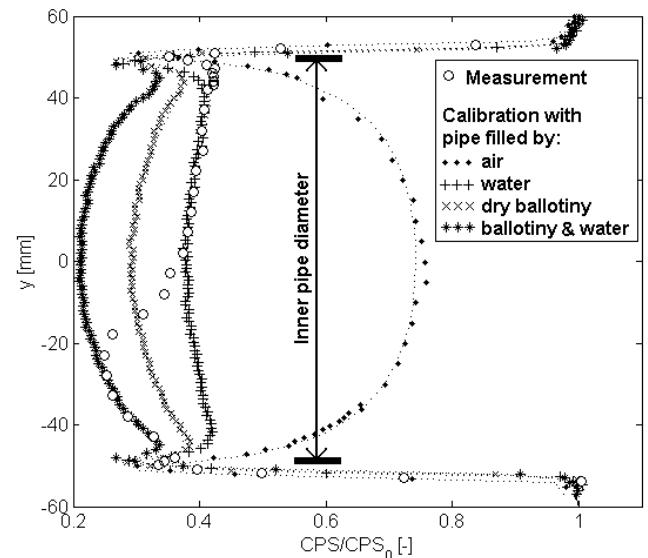


Figure 3: Vertical profile of normalized *CPS* for pipe with water flowing above eroded surface of stationary deposit. The profile is plotted together with a calibration data.

Data processing

Evaluation of profile of chord-averaged densities

A direct output of measurement at specified position and specified angle of inclination is a count N of detected photons with energy within predefined interval close to the emissive energy of the gamma ray source. The count of photons N is divided by measuring time period t to obtain *CPS* (Counts Per Second). Attenuation of gamma-ray intensity is characterized by value of *CPS* normalized by the referential value CPS_0 measured in the case of no object (no attenuation) between source and detector. This ratio is than compared with the calibration data measured with the pipe filled by the material of known density. The same

material as that used in experiment should be used for calibration. Figure 3 shows the typical profile of normalized *CPS* plotted together with calibration data. Data were measured in vertical centerline of horizontal steel pipe with stationary deposit of glass particles (ballotini) partially eroded by the flow of water above the deposit. Calibrations were made for the empty pipe and with the pipe filled by water, dry ballotini and ballotini with water. Actual chord-averaged density $\bar{\rho}_m$ is interpolated using exponential fit of calibration points at each position y .

Evaluation of local densities

The paragraph above describes how to process parallel projections data to obtain profile of chord-averaged densities. Local densities can be evaluated using computer tomography (CT) principles when the parallel projection measurements are carried out for several positions at radial positioning drive and thus for different angles of inclination. There are a number of methods used for image reconstruction in CT (Kak & Slaney, 1988). The choice of specific method depends on number of projections, desired accuracy, computational effort and nature of phenomena to be imaged by CT. As one projection measurement is rather time consuming we are limited by the total count of projections. On the other hand we are not limited by the time requirements of data evaluation. Rather continuous changes in local densities with no abrupt steps can be expected for the flow of settling slurry in pipe. Up to now we have tested two simple methods of density field reconstruction. The fact that unknown densities cover circular area of pipe cross-section can be easily reflected by the both methods. Moreover, they don't require any restriction on constant spacing of linear projections and angles of inclination on radial positioning drive. The first method is based on an approximation of density distribution $\rho(x, y)$ by the piecewise linear function defined in cells of a triangular mesh. Unknown densities ρ_i ($i = 1, \dots, N_U$) are stored in mesh nodes (Figure 4).

The second method approximates the density distribution by the two-dimensional polynomial function defined as:

$$\rho(x, y) = \sum_{i=0}^n \sum_{j=0}^m a_{ij} \cdot x^i \cdot y^j, \quad (2)$$

where x and y are defined in Figure 4, a_{ij} are unknown coefficients and n, m are degrees of the polynomial. Both methods are applied in a very similar way. For each projection the approximation ($\rho(x, y)$) is integrated along the beam length within the pipe cross-section. The chord-averaged density $\bar{\rho}$ is expressed from result of integration as a linear combination of unknown densities ρ_i or

unknown coefficients a_{ij} . Finally, this linear combination is set to be equal to density evaluated from measurement:

$$\bar{\rho} = \frac{1}{L} \int_0^L \rho(x, y) dl = \bar{\rho}_m, \quad (3)$$

For N_M projections one obtains N_M linear equations including N_U unknowns depending on the mesh size or the degree of the polynomial (2). We use $N_M > N_U$ to suppress influence of measuring errors. Then the solution is found employing the least square method.

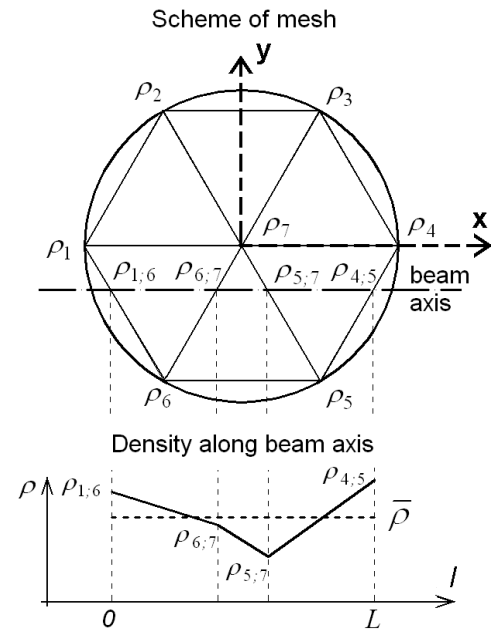


Figure 4: Piecewise linear approximation of density distribution in triangular mesh.

Experimental results

Chord-averaged concentrations

Profiles of chord-averaged concentrations of solid phase were calculated from chord-averaged densities and known density of fluid (water, $1000 \text{ kg}\cdot\text{m}^{-3}$) and solid particles (glass, $2460 \text{ kg}\cdot\text{m}^{-3}$). Figures 5 shows vertical concentration profiles of ballotini B8 (median size diameter = 0.53 mm , settling velocity = $7.2 \text{ cm}\cdot\text{s}^{-1}$) in a horizontal steel pipe for different average mixture velocities V_m (velocity in the entire pipe area including possible stationary deposit). Maximum possible volumetric concentration of 62% was obtained from extra experiment and it is also plotted. It can be seen how the particles tend to settle when the velocity of flow decreases. Stationary deposit was observed visually for profiles in Figure 5b. Virtually linear profile can be deduced from measurement within the high concentrated shear layer above the bed. Height of the shear layer rises with the flow velocity. This agrees well with the previous observations (e.g. Pugh & Wilson 1999, Matoušek 2009) made under the similar conditions.

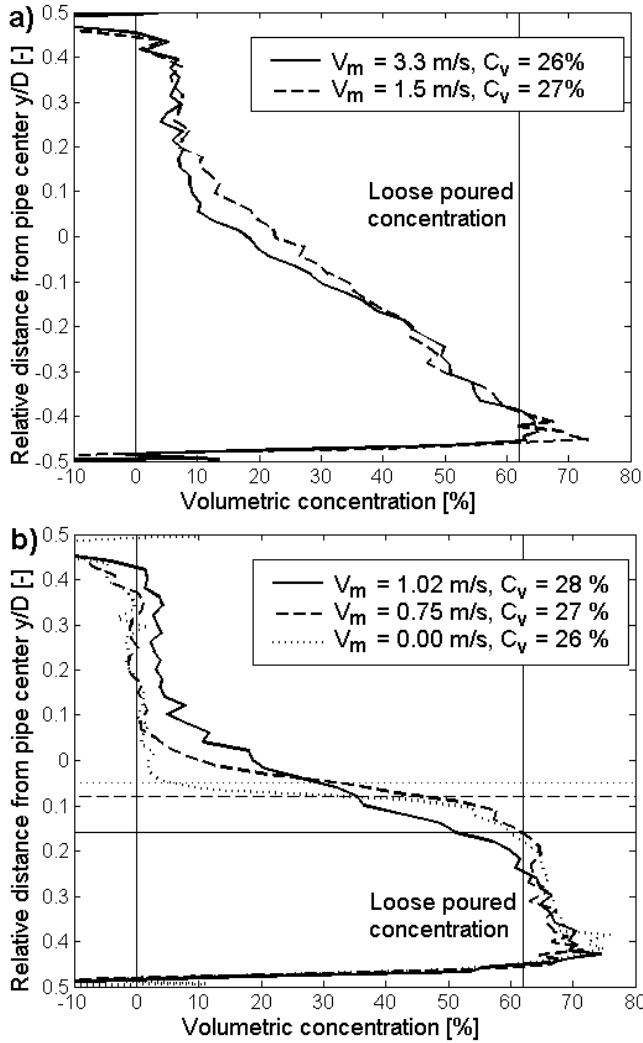


Figure 5: Vertical concentration profiles in horizontal pipe for different average mixture velocities V_m . a) no stationary deposit was observed, b) stationary deposit was observed (horizontal lines show position of deposit surface).

Profiles in Figure 5 also demonstrate the limitation of the method. Unrealistic values of concentration are obtained for positions y above the value of $|y/D|=0.4$. This can be explained by the rapid change in geometrical configuration (ratio of beam path length within the pipe and path length in the pipe wall) near the pipe wall causing the procedure of data evaluation sensitive to errors in projection position reading.

The average volumetric concentrations C_v in Figure 5 are results of integrating carried out on vertical concentration profiles. Unfortunately, no additional independent measurement is available to check values of C_v . The values of the delivered concentration (measured using the sampling tank) differ from C_v due to the phase slip in flow.

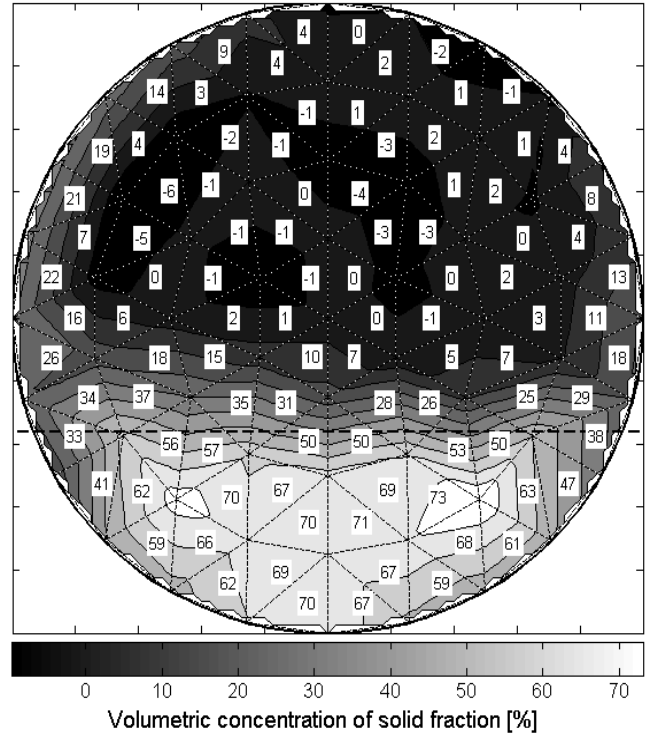


Figure 6a: Distribution of local concentration evaluated in triangular mesh (the dotted lines). Bold dashed line shows the level of deposit surface observed visually at the pipe wall.

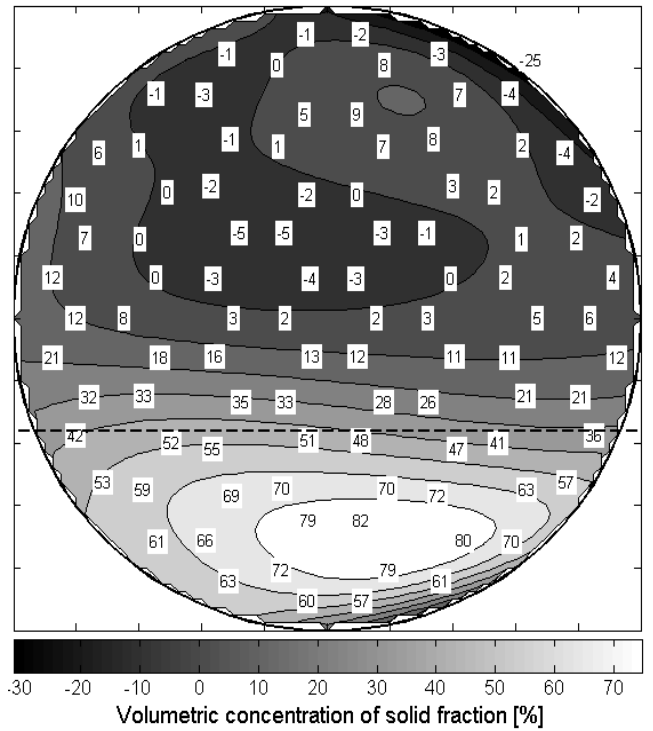


Figure 6b: Distribution of local concentrations evaluated from polynomial expression (2) with $n = 3, m = 6$. Bold dashed line shows level of deposit surface observed visually at the pipe wall.

On the other hand, C_v values vary only slightly within the entire range of measured velocities. This corresponds well with the fact that all profiles were measured for the same total amount of ballotini in the test loop.

Distribution of local concentrations

Taking into account the large uncertainty in measurement for projections near the pipe wall, only projections up to distance of $0.40D$ from the pipe centre are included in the procedure.

Figure 6 shows the distribution of local concentrations evaluated from the measurement with flow of water and ballotini TK0810 (median size diameter = 0.90 mm, settling velocity = 15 cm.s⁻¹) in a horizontal steel pipe of inner diameter of 100 mm. The average mixture velocity was $V_m = 1.02 \text{ m} \cdot \text{s}^{-1}$. Parallel projections step was five millimetres and the step of radial positioning drive was ten degrees, so the total number of projections included in CT procedure was approximately 340. According to actual position the number of 14000 – 40000 pulses was counted during the 16 s long measuring period of one projection. The stationary deposit was observed visually in the transparent section of pipe. As could be expected the polynomial expression (Figure 6b) provides more smooth distribution but it fails particularly near the wall (see the top right section in Figure 6b). Piecewise linear expression (Figure 6a) doesn't suffer by so much extreme values near the wall. Although the near wall region is also problematic the piecewise linear expression generally describes the concentration map more realistically. The both expressions result into the high concentrations near the left side of a pipe indicating that the problem is not in CT but in the measured data.

Measuring errors

Factors influencing accuracy

As experimental results presented above show the radiometric method of density measurement produces some errors particularly in the near wall regions. The main sources of inaccuracy were identified as follows.

- Emission of gamma-ray photons and their detection as pulses is in principle random process which can be described by Poisson distribution. Therefore detected CPS is corrupted by a random error with the normal distribution and standard deviation σ_{CPS} given by

$$\frac{\sigma_{CPS}}{CPS} = \frac{1}{\sqrt{CPS/t}} \quad (4)$$

- Although the gamma ray beam is collimated it can't be considered as narrow as the collimator opening. Due to a scattering of photons in an investigated mater some portion of detected photons always remains that passed through the

volume less or more far from the source-detector axis. This can be reflected in simplified form by assuming certain distribution of ray intensity across the beam. Generally, the wider distribution the worse spatial resolution of the method could be expected.

Our tests showed that 80 percent of the ray intensity travellers within the region of 1 mm from beam axis in the case of source without collimation. If the collimator with 0.75 mm – wide opening is mounted at source, the portion of photons increases up to 94 percent.

- Linear positioning drive was found to set a position with an error characterized by standard deviation of $\sigma_p = 0.32 \text{ mm}$. These errors affect accuracy of density evaluation from calibration data (Figure 3) as well as the reconstruction of local concentration map.
- Standard deviation of $\sigma_a = 0.25 \text{ deg}$ was estimated for errors in reading of angle of radial positioning drive inclination.
- Some inaccuracy is naturally related with selected method of evaluation of density distribution. Both methods presented in this paper describe the distribution in more details if the mesh is finer or degree of polynomial expression higher. On the other hand this is true only if the count of projections is consequently increased.

Possibilities of radiometric method optimisation

As the radiometric measurement and associated calculations are corrupted by random errors, evaluation of benefits of any improvement has to be proved statistically based on a large number of identical experiments. Real experiments are too time consuming, hence the numerical simulations of experiments were performed taking all uncertainties mentioned above to account.

The Figure 7b shows the profile of standard deviations of density σ_p simulated for the typical measuring conditions (i.e. beam collimated only at detector, measuring time period for one projection $t = 16 \text{ s}$, $CPS_0 = 1500 \text{ s}^{-1}$ and density profile defined in the Figure 7a).

An influence of gamma-ray intensity distribution across the beam was tested. Standard deviations of density were simulated with the beam collimated at both source and detector and compared with the deviations calculated for standard conditions (Figure 7c). As the density profile defined in the Figure 7a changes gradually, the benefit of better spatial resolution is not apparent. Standard deviation is even increased near the pipe wall where the higher spatial resolution probably results in the higher sensitivity to the errors in position reading. The same was observed also for the case of infinitely narrow beam.

The influence of errors in reading of position of linear positioning drive is clearly demonstrated in the Figure 7d. If the simulation with no errors in position reading is

performed, standard deviation of density decreases considerably near the pipe walls.

The random fluctuation in emission and detection of gamma-ray photons is identified as the most important source of errors by the Figure 7d. If the measuring time for one projection is increased, the standard deviation of density decreases considerably. The same can be achieved with the source with higher activity.

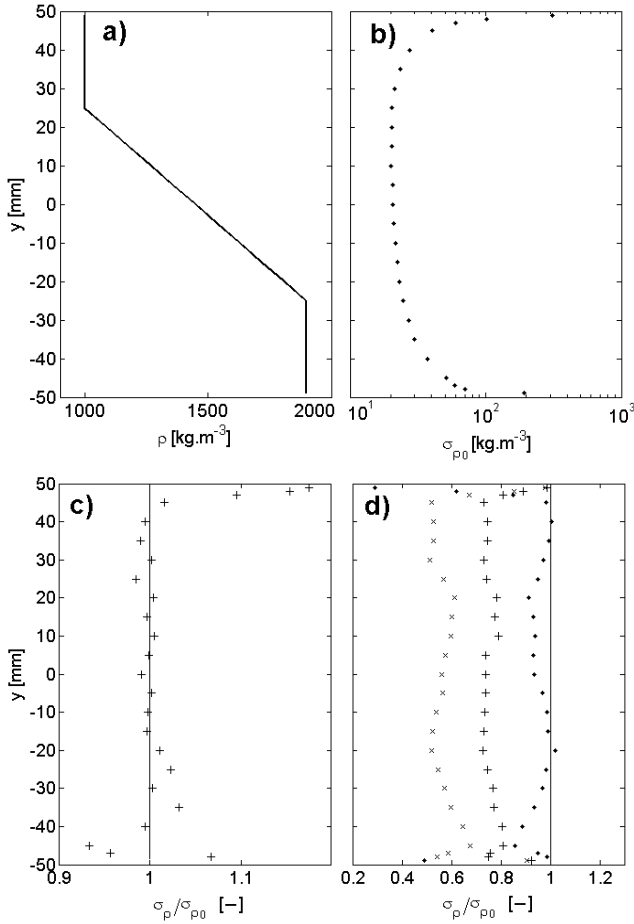


Figure 7: a) definition of density distribution used for numerical experiments, b) standard deviation of density evaluated from simulations under the standard conditions, c) influence of gamma-ray intensity distribution across the beam, d) influence of errors in linear positioning drive reading (\cdot), influence of random fluctuation of emission and detection of gamma-ray photons (measuring time period t : 30 s (+), 60 s (x)).

CONCLUSIONS

Radiometric devices were used for measuring density distribution in a slurry pipe of the experimental test loop at the Institute of Hydrodynamics in Prague. Measurements of vertical profiles of chord-averaged densities in the flow of water carrying solid particles provide valuable information for better understanding of principles of flows of settling slurries. Furthermore, radiometric devices are used to acquire data suitable for processing using computational

tomography. Hence, maps of local densities and concentrations can be reconstructed for a pipe cross-section. Up to now, two simple methods for map reconstruction were tested. The results are reasonable although reconstructed concentration maps exhibit some artificial artefacts particularly near the pipe wall. More sophisticated methods of map reconstruction will be tested to solve this problem.

A spatial resolution of the radiometric devices has been found sufficient for the application in flows with gradually changing density distribution. The random fluctuation of emission and detection of gamma-ray photons is identified as the most important source of errors affecting the method accuracy.

Acknowledgement

The research has been supported by the Czech Science Foundation through the grant project No. 103/09/0383.

References

- Hampel, U., Bieberle, A., Hoppe, D., Kronenberg, J., Schleicher, E., Sühnel, T., Zimmermann, F., and Zippe, C. (2007). High resolution gamma ray tomography scanner for flow measurement and non-destructive testing applications. *Review of Scientific Instruments*, 78(10), pp. 103704-1 - 103704-9.
- Hjertaker, B.T. and Johansen, G.A (2008). High speed gamma-ray tomography for hydrocarbon flow Applications. *An International Conference on the Applications of Computerized Tomography*. AIP Conference Proceedings, Vol. 1050, pp. 163-174.
- Kak, A.C. and Slaney, M. (1988). *Principles of Computerized Tomographic Imaging*, IEEE Press.
- Krupička, J., and Matoušek, V. (2011). First experimental experience with new laboratory slurry loop. *Proceedings of International Freight Pipeline Society Symposium*, Madrid, Spain, pp. 147-154.
- Lee, N.Y., Jung, S.H., and Kim, J.B. (2009). Evaluation of the measurement geometries and data processing algorithms for industrial gamma tomography technology. *Applied Radiation and Isotopes*, 64, pp. 141-1444.
- Matoušek, V. (1997). *Flow mechanism of sand-water mixtures in pipelines*. Doctoral thesis. Delft University Press, the Netherlands.
- Matoušek, V., 2009. Concentration profiles and solids transport above stationary deposit in enclosed conduit. *Journal of Hydraulic Engineering*, 135(12): 1101-1106.
- Pugh, F.J., (1995). *Bed-load velocity and concentration profiles in high shear stress flows*. PhD thesis. Queen's University at Kingston, Canada.
- Pugh, F.J., and K.C. Wilson, 1999. Role of the interface in stratified slurry flow. *Powder Technology*, No. 104, pp. 221-226.
- Przewlocki, K., et al (1979). A radiometric device for the determination of solids concentration distribution in a pipeline. *Proceedings of Hydrotransport 6*, Cantenbury, UK.